

# Calculation of the electrostatic field distribution formed by the generator of the off-electrode plasma

M.A. Markushin<sup>1</sup>, V.A. Kolpakov<sup>1</sup>, S.V. Krichevskiy<sup>1</sup>

<sup>1</sup>Samara National Research University, 34 Moskovskoe Shosse, 443086, Samara, Russia

## Abstract

A calculation of the electrostatic field distribution in the electrode system of a high-voltage gas-discharge device is made. The application of the conformal mapping method in order to obtain an analytical description of the of equipotentials and field lines distribution is described. The figures of the electrostatic field distribution are calculated, which made it possible to determine their relationship with the cathode-anode distance, the voltage at the electrodes and the hole diameter in the anode of the gas discharge device. The electrostatic field distribution of the device forming the off-electrode plasma is analyzed.

Keywords: plasma; high-voltage gas discharge; equipotentials; field lines; conformal mapping; the Schwarz-Christoffel integral

## 1. Introduction

The off-electrode gas-discharge plasma formed by a high-voltage gas discharge is used for plasmachemical etching of quartz, for preparing Ohmic contacts of semiconductor elements, cleaning the surfaces of semiconductor and dielectric substrates, contacts of small-size relays [1-4]. The high uniformity of the charged particles flow in the region of the gas discharge cross section and the independence of the discharge parameters from the dimensions of the treated area [5, 6] causes the wide propagation of this discharge. These advantages are a consequence of the singularity of the lines of the force and equipotentials distribution of the off-electrode plasma generator [7-9]. In turn, of the electrostatic field distribution depending on the design parameters determines the physics of the charged particles interaction processes with atoms and molecules of the residual gas. Existing publications contain no information on the relationship between such parameters and the electrostatic field distribution. Due with the laboriousness of the experimental study of this problem the computational model is proposed for the field distribution in the electrode system of a gas-discharge device.

## 2. Calculation of electrostatic field distribution of the off-electrode plasma generator

A high-voltage gas discharge is formed only in the area of the anode hole [8]. Outside this area, the electrode system design is a flat capacitor with uniform field distribution. Therefore, the design of a gas discharge device can be modeled by an electrode system in which the cathode and anode area outside of the electric field inhomogeneity are removed to infinity (fig. 1).

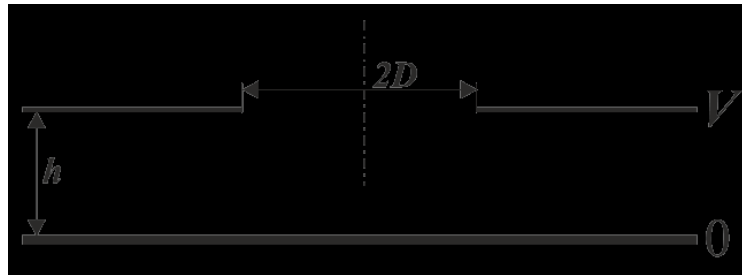


Fig.1. Schematic diagram of a device forming a high-voltage gas discharge:  $h$  is the anode–cathode distance,  $D$  is the radius of the anode orifice,  $V$  is the anode potential,  $0$  is the cathode potential.

Obtaining an analytical description of the distribution of the electrostatic field in the hole area in the anode is hampered because field unevenness. To simplify such a problem, it is necessary to reduce it to the solution of the two-dimensional task, which will make it possible to simplify considerably the calculation of field lines and equipotentials by finding the complex potential for the canonical domain with a simple form of boundaries [10, 11]. Since the thickness of the anode has a value in the range of up to 0.5 mm, its influence on the formation of the electrostatic field is insignificant, because this thickness is smaller than the cathode-anode distance ( $h$  to 10 mm). Therefore, this quantity can be neglected.

The symmetry principle of the conformal mapping method allows us to consider only the right part of the obtained electrode system for the solution of the posed task by realizing the projection of the electrodes on the complex plane  $Z$ . This projection is shown in Fig. 2 (polygon)  $A_1A_2A_3A_4$ .

Simulation of the electrostatic field begins with finding the conformal mapping  $Z = f(\omega)$  of the upper half-plane  $\text{Im}\omega > 0$  to the region of the  $Z$  field with the electrodes  $A_1A_2$  (cathode),  $A_3A_4$  (anode) (fig. 2) with internal angles  $\alpha_k\pi$  at the vertices. Then an additional mapping  $\xi = f(\omega)$  of the half-plane  $\omega$  onto a strip  $0 < \text{Im}\xi < V$  with internal angles  $\beta_k\pi$  at the vertices (fig. 3).

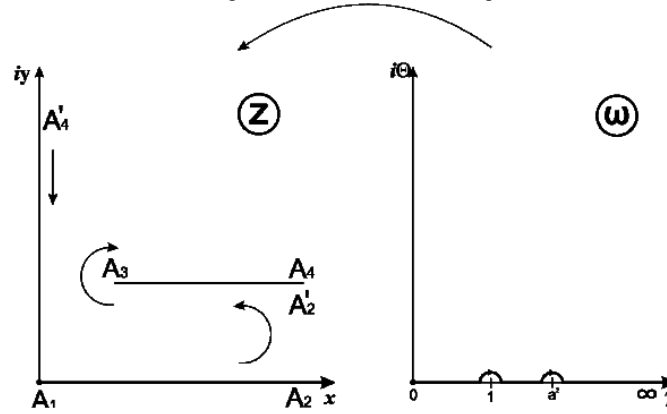
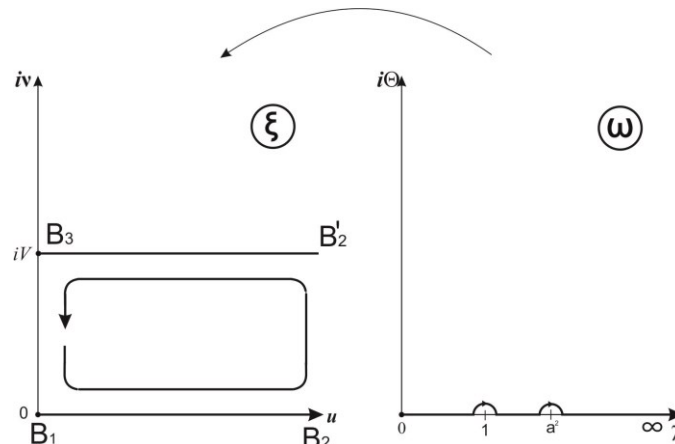


Fig.2. Diagram of the half-plane mapping onto plane (the electrode system).


 Fig.3. Diagram of the additional mapping of the half-plane  $\text{Im } w > 0$  onto the strip  $0 < \text{Im } \xi < V$ .

At the first stage, the vertices  $A_1 A_2 A_3 A_4$  of the  $Z$ -plane are associated with certain points of the real axis of the plane  $w$ . According to the theorem of uniqueness of a conformal mapping for a present correspondence of three arbitrarily chosen boundary points, for example,  $0, 1, \infty$ , we can obtain the correspondence [11]:

$$\begin{array}{cccc} A_1 & A_2 & A_3 & A_4 \\ 0 & 1 & a^2 & \infty \end{array}$$

According to the technique developed in [10-12], the angles  $\mu_k$  are determined, which complement the internal angles  $\alpha_k$  at the vertices of the quadrangle  $A_1 A_2 A_3 A_4$  to  $\pi$ . Considering the inner region of a quadrilateral and moving in the positive direction of traversing its boundary, i.e. counterclockwise, we find the angles:  $\mu_1 = 1/2$  ( $\alpha_1 = 1 - \mu_1 = 1/2$ );  $\mu_2 = 1$  ( $\alpha_2 = 1 - \mu_2 = 0$ );  $\mu_3 = -1$  ( $\alpha_3 = 1 - \mu_3 = 2$ );  $\mu_4 = 3/2$  ( $\alpha_4 = 1 - \mu_4 = -1/2$ ).

To find the mapping function of a domain bounded by a polygon  $A_1 A_2 A_3 A_4$  the Schwarz-Christoffel integral [11] is used:

$$Z = C \int_{\omega_0}^{\omega_1} (\omega - a_1)^{\alpha_1 - 1} (\omega - a_2)^{\alpha_2 - 1} \dots (\omega - a_n)^{\alpha_n - 1} d\omega + C_1, \quad (1)$$

In the expression (1) instead of  $a_1 - a_n$  we substitute the corresponding points  $0, 1, a^2, \infty$ . According to [10], the factor related to the vertex  $a_4$  in the Schwarz-Christoffel integral is omitted, since  $a_4 = \infty$ .

In this case, the expression (1) has the form:

$$Z = C \int_0^{\omega} \omega^{-1/2} (\omega - 1)^{-1} (\omega - a^2) d\omega + C_1 = C \int_0^{\omega} \frac{(\omega - a^2)}{(\omega - 1)\sqrt{\omega}} d\omega + C_1$$

Let  $\omega = x^2$ , then:

$$Z = C \int_0^{\sqrt{\omega}} \frac{(x^2 - a^2)}{(x^2 - 1)x} dx^2 + C_1 = 2C\sqrt{\omega} + C(a^2 - 1) \ln \frac{1 + \sqrt{\omega}}{1 - \sqrt{\omega}} + C_1. \quad (2)$$

The value of the constant coefficient  $C_1$  is determined from the correspondence of the points  $A_1 \leftrightarrow 0$ , which allows us to write the equation:

$$Z = 2C \cdot 0 + C(a^2 - 1) \ln \frac{1 + \omega}{1 - \omega} + C_1 = C_1 = 0.$$

The transition from the lower electrode to the upper one, corresponding to the transition of the ray  $A_1A_2$  to the ray  $A_2A_3$  (fig. 2), allows us to determine the constants  $a^2$  and  $C$ . As a result, the function receives an increment:

$$\Delta Z = ih. \quad (3)$$

In addition, with such a small increment  $\Delta\omega$ , the increment of the first term in (2) is also small because of the continuity of this term at  $\omega = 1$ . Taking into account that the argument varies from  $\pi$  to 0 as we go around the point  $\omega = 1$ , the increment of the second term has the form:

$$\ln \frac{1 - \sqrt{\omega}}{1 + \sqrt{\omega}} = \ln(r) - \ln(re^{i\pi}) = -i\pi.$$

This allows us to write the expression:

$$\Delta Z = \lim_{r \rightarrow 0} [2C\sqrt{\omega} - C(1 - a^2) \ln \frac{1 - \sqrt{\omega}}{1 + \sqrt{\omega}}]_{\omega=r}^{\omega=re^{i\pi}} = C(1 - a^2)(-i\pi). \quad (4)$$

Equating (3) and (4), we obtain:

$$ih = C(a^2 - 1)i\pi.$$

Thus, the change of the coefficient value  $a^2$  can be described by the equation:

$$a^2 = \frac{h}{C \cdot \pi} + 1. \quad (5)$$

The correspondence of the points  $a^2$  and  $A_3$  makes it possible to transform expression (2) to the form:

$$D + ih = \frac{2 \times ha}{(a^2 - 1) \times \pi} + \frac{h}{\pi} \ln \left( -\frac{a+1}{a-1} \right) = \frac{2 \times ha}{(a^2 - 1) \times \pi} + \frac{h}{\pi} \ln \left( \frac{a+1}{a-1} \right) + \frac{h}{\pi} i\pi,$$

$$D = \frac{2 \times ha}{(a^2 - 1) \times \pi} + \frac{h}{\pi} \ln \left( \frac{a+1}{a-1} \right).$$

Whence we obtain the following equality:

$$\exp \left( D \frac{\pi}{h} - \frac{2 \times a}{a^2 - 1} \right) = \frac{a+1}{a-1}. \quad (6)$$

Given specific values of  $D = 0.9$  mm,  $h = 1.2$  mm, we can obtain a solution of the transcendental equation (6) and find the value of the constant  $a^2 = 4.179$ . Substituting it in (5), we obtain  $C = 0.24$  mm.

As a result, the function realizing the conformal mapping of the half-plane  $\omega$  onto the plane  $Z$  has the form:

$$Z = 2C\sqrt{\omega} + \frac{h}{\pi} \ln \left( \frac{1 + \sqrt{\omega}}{1 - \sqrt{\omega}} \right). \quad (7)$$

Thus, expressions (5), (6) allow us to find a constant  $C$  whose value depends on the design parameters  $D$  and  $h$ .

At the second stage, an additional mapping of the half-plane  $\text{Im}\omega > 0$  is applied to the strip  $0 < \text{Im}\xi < V$  with cuts along the corresponding rays (fig. 3). In this case we have a capacitor with infinite plates in the plane  $\xi$ .

Considering only the right triangle with vertices  $B_1B_2B_3$  because of the electrode design symmetry, we put the points 0, 1,  $\infty$  lying on the real axis  $\omega$  in correspondence to these vertices [11]:

$$\begin{array}{ccc} B_1 & B_2 & B_3 \\ 0 & 1 & \infty \end{array}$$

The inner angles  $\beta_k$  at the vertices of the triangle  $B_1B_2B_3$  and the angles  $\mu'_k$ , that complement the angles  $\beta_k$  to  $\pi$ , are defined similarly to  $\alpha_k, \mu_k$ :  $\mu'_2 = 1$  ( $\beta_2 = 1 - \mu'_2 = 0$ );  $\mu'_3 = 1/2$  ( $\beta_3 = 1 - \mu'_3 = 1/2$ );  $\mu'_1 = 1/2$  ( $\beta_1 = 1 - \mu'_1 = 1/2$ ).

The obtained values  $\beta_1 = 1/2, \beta_2 = 0, \beta_3 = 1/2$ , ensure equality  $\sum_{i=1}^3 \beta_i = 1$ , which confirms the correctness of the sought angles values according to [11].

An additional conformal mapping is also determined by the Schwarz-Christoffel integral [10]:

$$\xi = C_2 \int_0^\omega \omega^{-1/2} (\omega - 1)^{-1} d\omega = C_2 \int_0^\omega \frac{d\omega}{(\omega - 1)\sqrt{\omega}} + C_3.$$

The introduction of the new variable  $\omega = u^2$  allows us to obtain the solution of the given integral:

$$\xi = 2C_2 \int_0^{\sqrt{\omega}} \frac{udu}{(u^2-1)u} + C_3 = -C_2 \ln \frac{1+\sqrt{\omega}}{1-\sqrt{\omega}} + C_3. \quad (8)$$

From the correspondence of the points  $B_1 \leftrightarrow 0$  according to the technique outlined above, there is a constant  $C_3$ .

$$\xi = -C_2 \ln \frac{1+\sqrt{0}}{1-\sqrt{0}} + C_3 = 0 + C_3,$$

$$C_3 = 0.$$

The constant  $C_2$  is defined similarly to the constant  $C$  in the first stage, namely, by traversal of the point  $\omega = 1$ , we get the increment

$$\Delta\xi = iV.$$

Since the increment of the argument changes from  $\pi$  to 0 upon traversal of the above point, the increment of function  $\xi$  corresponds to the expression:

$$\Delta\xi = \lim_{r \rightarrow 0} [-C_2 \ln \frac{1+\sqrt{\omega}}{1-\sqrt{\omega}}]_{\omega=r}^{\omega=re^{i\pi}} = -C_2(-i\pi) = C_2 i\pi,$$

which allows us to obtain equality:

$$iV = C_2 i\pi.$$

Solving this equality, we define  $C_2$  :

$$C_2 = \frac{V}{\pi}.$$

The final function conformally mapping the half-plane  $\omega$  to the strip  $0 < \text{Im}\xi < V$  has the form:

$$\xi = \frac{V}{\pi} \ln \frac{1+\sqrt{\omega}}{1-\sqrt{\omega}} = \frac{2V}{\pi} \text{arcth}\sqrt{\omega}. \quad (9)$$

Using (7) and (9), we obtain a system of equations:

$$\begin{cases} Z = 2C\sqrt{\omega} + \frac{h}{\pi} \text{Ln} \left( \frac{1+\sqrt{\omega}}{1-\sqrt{\omega}} \right) \\ \xi = \frac{2V}{\pi} \text{arcth}\sqrt{\omega} \end{cases} \quad (10)$$

From (10) we find

$$Z = 2C \cdot \text{th} \frac{\xi\pi}{2V} + \frac{h}{\pi} \ln \left( \frac{1 + \text{th} \frac{\xi\pi}{2V}}{1 - \text{th} \frac{\xi\pi}{2V}} \right) = 2C \cdot \text{th} \frac{\xi\pi}{2V} + \frac{h}{V} \xi. \quad (11)$$

By separating the real and imaginary parts of equation (11), the parametric equations of lines of equal potential and field lines of force are found. After separation, we obtain a system of equations describing the coordinates of the electric field distribution in the electrode system of a gas-discharge device:

$$\begin{cases} x = \frac{hu}{V} + 2C \frac{\text{sh} \frac{u\pi}{V}}{\text{ch} \frac{u\pi}{V} + \cos \frac{v\pi}{V}} \\ y = \frac{hv}{V} + 2C \frac{\sin \frac{v\pi}{V}}{\text{ch} \frac{u\pi}{V} + \cos \frac{v\pi}{V}} \end{cases}. \quad (12)$$

Substituting the parameters  $h, V, D$  into the expressions (5), (6) and system (12) and changing the values of the variables  $v$  and  $u$  with the necessary step, we can determine the number of the field lines and equipotential distribution (fig.4 and fig.5).

Changing the voltage at the electrodes does not lead to a change in the field configuration, but it affects the energy of charged particles. Thus, the equations system (12) allows to obtain the electrode system configuration to form the required electric field by varying the parameters  $h, V, D$ .

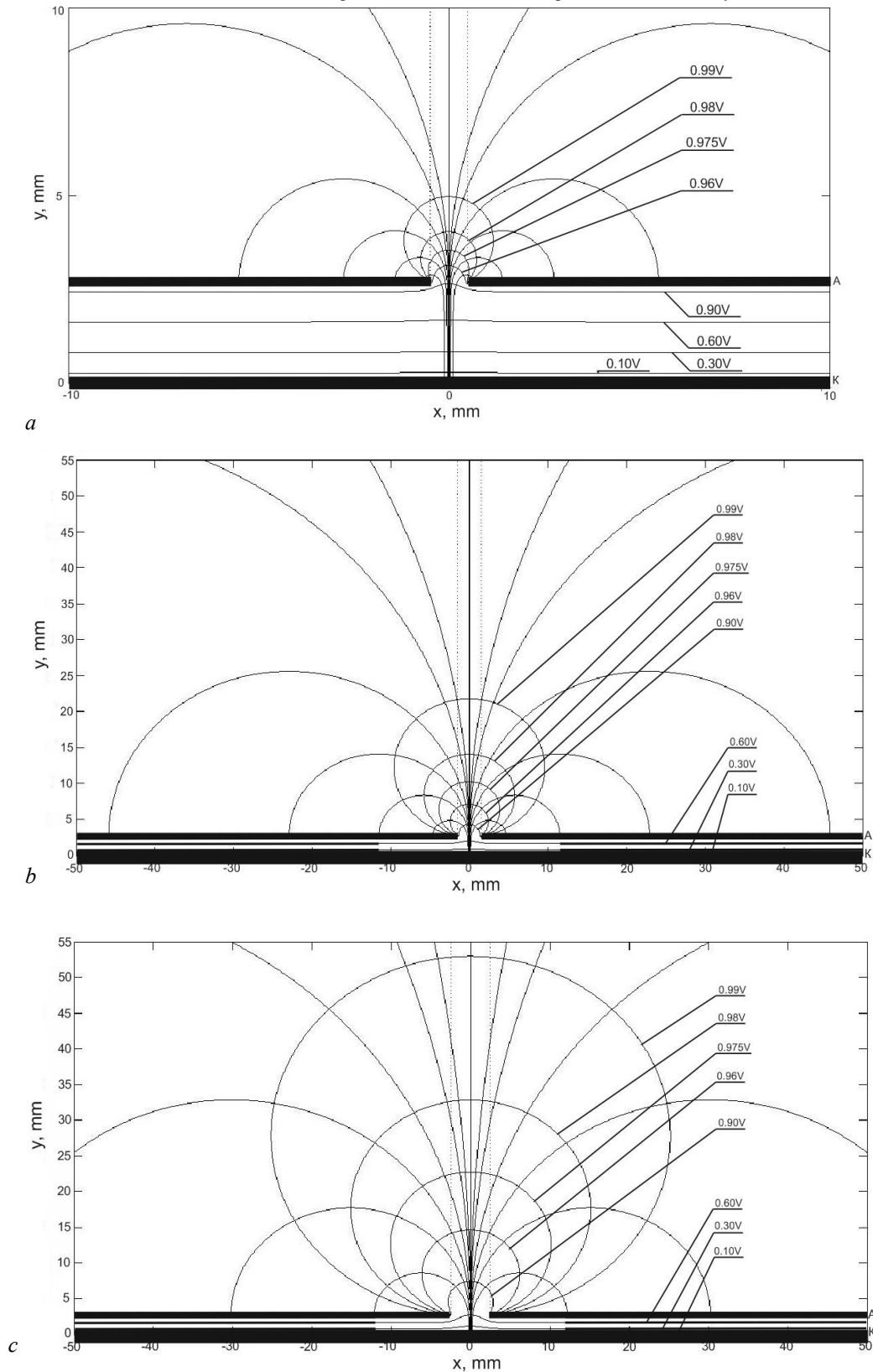


Fig.4. Field lines and equipotentials distribution in the electrode system of the gas-discharge device obtained by the equations system (12):  $a - h = 2.7$  mm,  $D = 1$  mm,  $V = 1200$  V;  $b - h = 2.7$  mm,  $D = 3$  mm,  $V = 1200$  V;  $c - h = 2.7$  mm,  $D = 5$  mm,  $V = 1200$  V.

### 3. Analysis of the field lines and equipotentials distribution

The initial coordinate ( $x = x_0, y = y_0 = 0$ ) of the rectilinear segment of the field line can be determined with the aid of the system (12), giving the values  $u = u_0$  and  $v_0 = 0$ . Then, searching further all the values of  $v = v_1 - v_n$  for which the coordinate  $x = x_0$  is constant, and the  $y$  varies in the limits  $y_1 - y_n$ . Further on, comparing the obtained maximum value of  $y_n$  with the mean free path of the electron  $k\lambda_e$  ( $k = 1, 2, 3$ ) and the potential at the given point with the ionization energy of the working gas atom (molecule)  $E_i$ , we verify the fulfillment of the condition for the emergence of a high-voltage discharge  $\gamma Q \geq 1$  [ 8 ] is, where  $\gamma$  is the number of electrons knocked by one ion from the cathode ( $\gamma$ -process),  $Q$  is the number of positive ions formed by the electron on the trajectory of its motion due to inelastic collisions with atoms and molecules of the working gas ( $\alpha$ -process). The energy

accumulated by the electron on the mean free path must be higher than the ionization energy of the working gas atom, and the energy of the positive ion bombarding the cathode must be sufficient for the emission of electrons necessary for sustaining the self-dependent discharge. Analogously, changing the values  $u = u_l - u_n$  for  $v_0 = 0$ , the corresponding  $x = x_l - x_n$  are determined. Further on, searching further values of  $v = v_l - v_n$  for each  $x$ , we find  $y = y_l - y_n = 0 - k\lambda_e$ . In other words, by repeating the comparison process, we can find all field lines with initial coordinates  $x_0, \dots, x_{\lambda_e}$ , on the rectilinear segments of which the ionization process takes place ( $\alpha$ -process), and, accordingly, the length of the cathode region  $\Delta x = 2x_{\lambda_e}$  where the electron emission from the cathode ( $\gamma$ -process) takes place [13].

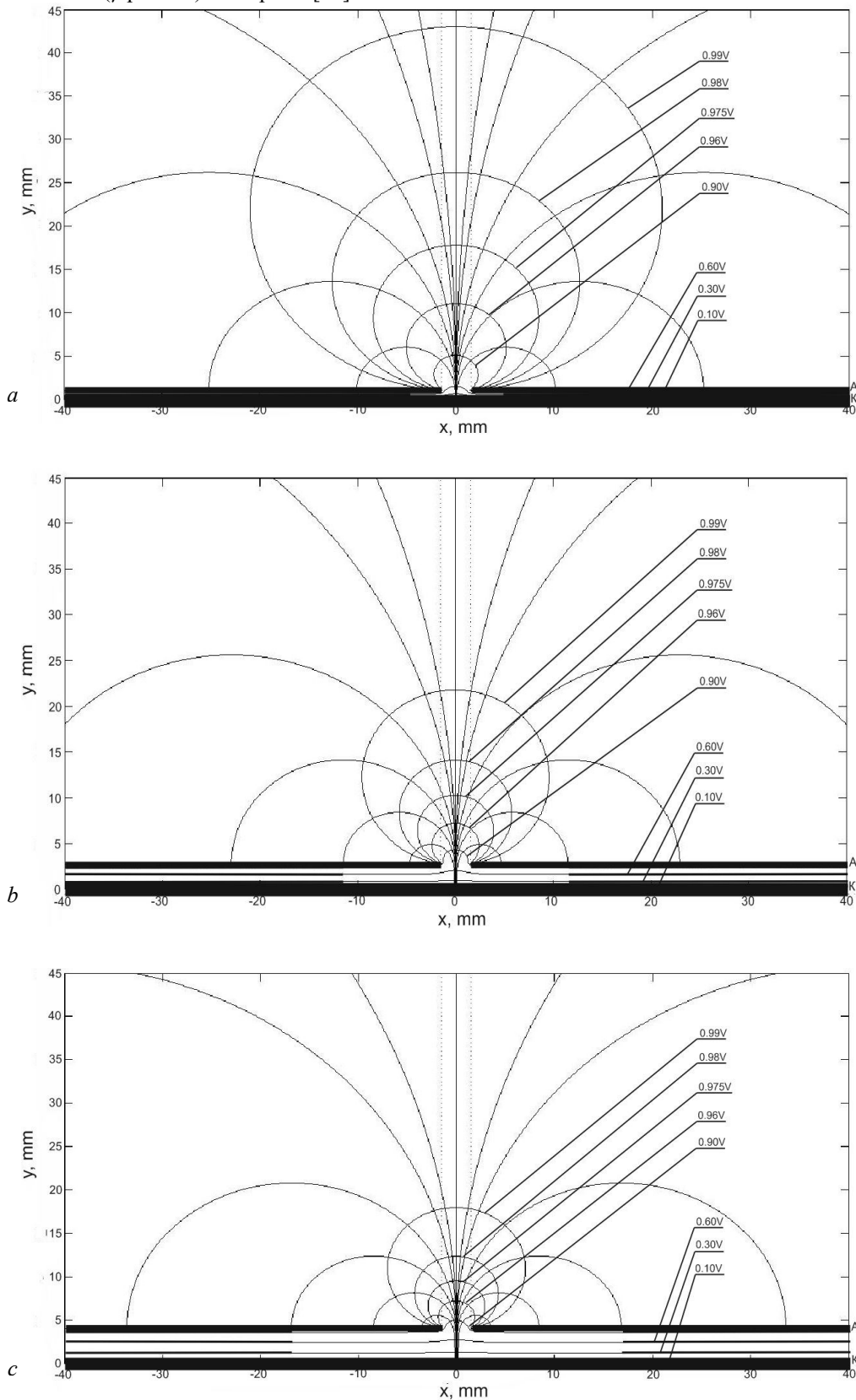


Fig.5. Field lines and equipotentials distribution in the electrode system of the gas-discharge device obtained by the equations system (12):  $a - h = 1$  mm,  $D = 3$  mm,  $V = 1200$  V;  $b - h = 2.7$  mm,  $D = 3$  mm,  $V = 1200$  V;  $c - h = 4$  mm,  $D = 3$  mm,  $V = 1200$  V.

In order to compare the maximum values of  $y_n$  with  $k\lambda_e$ , it is necessary to find the mean free path of an electron. Using the expression  $\lambda_e = l/(N\sigma_e)$  [14], we obtain the value 0.203 cm, which makes it possible to determine  $\Delta x = 318 \mu\text{m}$ . The calculated value of  $\Delta x$  correlated well with the experimental data of [9], namely, the size of the region on the cathode surface with intense sputtering by positive ions is 300  $\mu\text{m}$  (fig. 6).

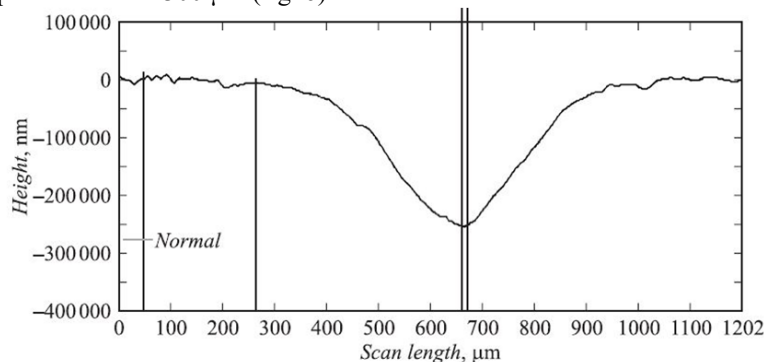


Fig 6. The profile of the etching pit on the surface of the cathode formed by positive ions.

This value is comparable with the size of the region  $\Delta x$  on which the rectilinear segments of field lines correspond to the value  $k\lambda_e$  and the condition for the emergence of an high-voltage discharge is observed.

#### 4. Conclusions

The parametric equations system presented in this paper makes it possible to simulate the of the field lines and equipotentials distribution in the electrode system of the off-electrode plasma generator and to monitor the dependence of this distribution on the design parameters of the system: the anode-cathode distance, the hole diameter in the anode, and also on the applied voltage at the electrodes. In addition, estimates are made in this paper: the length of the rectilinear segments of the field lines on which the condition is satisfied, the size of the cathode spot  $\Delta x$  within which the  $\gamma$  process is realized. The discrepancy between the calculated value and the experimental value does not exceed 6%, which indicates that the model corresponds to the actual physical processes occurring in the electrode system of a high-voltage gas discharge. Therefore, it becomes possible to optimize the devices design forming the off-electrode plasma without costly experimental investigations.

#### Acknowledgments

This work was supported by grants from the President of the Russian Foundation for State Support of Young Russian Ph.D. Scientists (MD-5205.2016.9) and the Russian Foundation for Basic Research (project no. 16-07-00494 A).

#### References

- [1] Komov AN, Kolpakov AI, Bondareva NI, Zakharenko VV. Electron-beam unit for soldering semiconductor devices. *Instruments and Experimental Techniques* 1984; 5: 218-220.
- [2] Kazanskiy NL, Kolpakov VA, Kolpakov AI. Investigation of the features of the anisotropic etching of silicon dioxide in plasma high-voltage gas discharge. *Microelectronics* 2004; 33(3): 209-224.
- [3] Kolpakov VA, Kolpakov AI, Krichevskiy SV. Ion-plasma cleaning of the low-power relay contacts surface. *Elektronnaya promyshlennost* 1996; 2: 41–44.
- [4] Kazanskiy NL, Kolpakov VA, Krichevskiy SV. Simulation of the cleaning process the surface of dielectric substrates in plasma formed by high-voltage gas discharge. *Computer Optics* 2005; 28: 80–86.
- [5] Kazanskiy NL, Kolpakov VA. Investigation of the mechanisms of low-temperature plasma formation by a high-voltage gas discharge. *Computer Optics* 2003; 25: 112–116.
- [6] Kazanskiy NL, Kolpakov VA, Kolpakov AI, Krichevskiy SV. Gas discharge devices forming directed flows of the off-electrode plasma. Part I. *Nauchnoe priborostroenie* 2012; 22(1): 13–18.
- [7] Soifer VA, Kazanskiy NL, Kolpakov VA, Kolpakov AI. Patent 2333619 Russian Federation, MPK H 05 H 1/24. Multi-beam gas-discharge plasma generator. Applicant and patent holder IPSI RAS N 2006121061; declared 13.06.06; published 10.09.08, bulletin. N 25; 5 p.
- [8] Kazanskiy NL, Kolpakov VA. Formation of an optical microrelief in off-electrode high-voltage gas discharge plasma. *M. : Radio and Communications*, 2009; 220 p.
- [9] Kolpakov VA, Kolpakov AI, Podlipnov VV. Formation of the off-electrode plasma in a high-voltage gas discharge. *Technical Physics* 2013; 83(4): 41–46.
- [10] Miroljubov NN, Kostenko MV, Levinshstein ML, Tihodeev NN. Calculation methods of electrostatic fields. M.: Vysshaja Shkola, 1963; 415 p.
- [11] Lavrent'ev MA, Shabat BV. Methods of the theory of functions of a complex variable / M.A. Lavrent'ev. M.: Nauka, 1973; 736 p.
- [12] Novgorodtsev AB, Fethiev AR, Fethieva IS. Application of complex variable function to calculation of electrostatic fields of irregular shape electrodes: a tutorial. Ufa: Ufimskij ordena Lenina aviacionnyj institut im. Sergo Ordzhonikidze, 1986; 82 p.
- [13] Raizer YuP. Gas discharge physics. M.: Nauka, 1987; 592 p.
- [14] Kudryavtsev AA, Smirnov AC, Tsendin LD. Physics of glow discharge: a tutorial. SPb.: Lan', 2010; 512 p.